ACS Energy LETTERS

http://pubs.acs.org/journal/aelccp

LETTER

From the Junkyard to the Power Grid: Ambient Processing of Scrap Metals into Nanostructured Electrodes for Ultrafast Rechargeable Batteries

Nitin Muralidharan,[†,‡,§] Andrew S. Westover,[†,‡,§] Haotian Sun,[‡] Nicholas Galioto,[‡] Rachel E. Carter,[‡] Adam P. Cohn,[‡] Landon Oakes,[†,‡] and Cary L. Pint*[,†,‡]

[†]Interdisciplinary Materials Science Program and [‡]Department of Mechanical Engineering, Vanderbilt University, Nashville, Tennessee 37235, United States

Supporting Information

ABSTRACT: Here we present the first full cell battery device that is developed entirely from scrap metals of brass and steel—two of the most commonly used and discarded metals. A room-temperature chemical process is developed to convert brass and steel into functional electrodes for rechargeable energy storage that transforms these multicomponent alloys into redox-active iron oxide and copper oxide materials. The resulting steel−brass battery exhibits cell voltages up to 1.8 V, energy density up to 20 Wh/kg, power density up to 20 kW/kg, and stable cycling over 5000 cycles in alkaline electrolytes. Further, we show the versatility of this technique to enable processing of steel and brass materials of different shapes, sizes, and purity, such as screws and shavings, to produce functional battery components. The simplicity of this approach, building from chemicals commonly available in a household, enables a simple pathway to the local recovery, processing, and assembly of storage systems based on materials that would otherwise be discarded.

The complexity of modern battery systems that involve highly processed and purified materials, air-sensitive materials, and/or flammable electrolytes sustains a multibillion dollar battery industry devoted to delivering safe, high energy density, and portable energy storage solutions.[1−3] However, the early development of the first known batteries hinged on a much different rationale, where readily accessible (bulk) materials were combined at local scales to store energy. An early example of this is the first (speculated) development of a battery known as the "Baghdad battery"[4] dating back to the first century BC that consists of a terracotta (ceramic) pot with a copper sheet and iron rod. More recent examples include the copper zinc system discovered by Volta[5] and the nickel iron battery developed by Edison,[6−8] both where common metals are immersed in simple electrolytes for local energy storage. Today, whereas bulk materials are readily available, achieving competitive high-performing battery materials requires processing control and materials not commonly available in a residential or household setting.

In this spirit, stationary (grid-scale) storage of energy presents a critical solution to the intermittency of a future power grid that builds from a high penetration of renewable power generation such as wind and solar.[9,10] However, a critical barrier to energy storage on the grid is the infrastructure needed for (low-cost) centralized storage systems, such as redox flow batteries, or pathways to implement high-cost metal ion batteries for distributed storage.[9,11] Other routes such as liquid metal batteries show promise,[12] but any route that significantly modifies the current centralized grid architecture poses a large barrier for practical incorporation into a future renewable grid system. On this note, as emerging manufacturing routes such as 3-D printing are aiming to transplant centralized industries onto local scales,[13−15] one may consider the feasibility for this vision to impact the future of stationary storage, especially given the historical framework in which batteries were developed. Could future consumers or communities have the capability to cost-effectively and safely produce batteries for stationary storage applications?

Received: July 25, 2016
Accepted: October 16, 2016
Published: October 17, 2016

Downloaded via IOWA STATE UNIV on January 20, 2019 at 13:32:39 (UTC).
See https://pubs.acs.org/sharingguidelines for options on how to legitimately share published articles.

© 2016 American Chemical Society

DOI: 10.1021/acsenergylett.6b00295
ACS Energy Lett. 2016, 1, 1034−1041

On this front, the side-effect of consumer-driven large-scale manufacturing is the depreciation of manufactured systems and eventual disposal of the material as waste. Scrap metals represent over 130 million tons of waste each year, with steels representing 84 million tons, aluminum representing 7.3 million tons, and brass (copper) representing 1.38 million tons a year.[16,17] Although scrap metal recycling is active in the United States and worldwide today,[18] there are still enormous amounts of scrap metal waste that are not recycled each year, including an estimated 17.5 million tons of steel,[19] and an estimated 1.15 million tons of copper/brass.[17] This is in part due to the lack of consumer benefits for scrap recycling and the high cost of single-stream recycling infrastructure. As steel and brass exist as multicomponent alloys and are present in nearly every household, a critical barrier to repurposing these materials rather than discarding them is the availability to carry out material processing in a common household environment. In this manner, chemical processing using anodization is particularly attractive because this technique requires low voltages, often builds from water-based environments, and can be leveraged to produce controllable nanostructured materials ideally suited for applications such as energy storage.[20−22] The anodization process for multicomponent alloys utilizes a voltage applied in a reactive electrolyte to electrochemically remove (and/or oxidize) one or more elemental species and has been demonstrated for a wide range of materials and applications. Specifically for energy storage applications, anodization has been shown as an excellent tool to process binary metal alloys, and especially NiTi alloys, into porous or nanotubular nickel oxide or titanium oxide materials with high specific energy storage capability compared to that of bulk metal oxides.[22,23] However, as of yet, anodization of complex multicomponent alloys such as steels or brass for the purpose of energy storage applications has never been explored. Unlike high-purity metals, these manufacturing alloys involve elemental additives that act to improve the material properties but complicate processing into a target metal oxide functional material. Nonetheless, the abundance of these metals from manufactured products makes these materials excellent scaffolds for practical investigations leading to energy storage materials.

In this work, we draw inspiration from the rationale and working materials of the original Baghdad battery and demonstrate a route where otherwise discarded scrap metals of brass and steels can be processed and combined to yield ultrafast rechargeable batteries. This builds upon an anodization process producing nanostructured electrodes from brass and cheap low-carbon steels that, when paired in aqueous electrolytes, exhibit nominal voltage ranging from 1 to 1.8 V, energy densities upward of 20 Wh/kg, and power densities up to 20 kW/kg. Further, we show that this idea can be transferred to metal scraps with various shapes, sizes, and purities, such as screws and shavings, which motivates the use of this processing strategy at local scales to generate functional energy storage capability from otherwise discarded metal objects.

A general scheme that elucidates the approach to transform scrap metals into ultrafast rechargeable batteries is shown in Figure 1. Importantly, the primary consideration when assembling two electrodes into a battery assembly is the total resulting operation voltage, which is dictated by the relative potential of the redox couples at the anode and the cathode. In this manner, the original Ni−Fe battery system developed by Edison has re-emerged in the research arena due to the moderate voltage (~1.5 V) and the capability to produce

Figure 1. Schematic representation of the process of developing the scrap metal battery with a photograph of one of two scrap metal jar batteries powering a blue LED.

nanostructured $Ni(OH)_2$ and Fe_xO_y structures readily from bulk materials.[7,24−26] However, whereas brass has never been studied as the basis for a battery electrode, CuO_x active materials (Cu is the primary component of brass) exhibit redox couples ranging from +0.2 to 0.6 V vs saturated calomel electrode (SCE) in aqueous KOH, which are very close to those for NiOH.[27,28] Compared to nickel metal electrodes, brass is significantly less toxic, more abundant as a metal, and cheaper (~$1.1 per lb versus ~$3.6 per lb, United States Scrap Register).[29] This led us to envision using low carbon steel, the most abundant scrap metal, as a source of iron oxide and brass, the third most abundant scrap metal, as a source of copper oxide and combining it with aqueous KOH electrolyte to produce a full cell battery with appropriate electrode potential pairing to produce a competitive energy storage platform. To generally demonstrate the function of this battery system, Figure 1 shows one of two scrap metal battery cells wired in series to light up a blue LED where the anodized brass and anodized steel electrodes can be clearly seen.

In this effort, the use of anodization is critical to transforming scrap metal into electrodes with a low environmental impact and additionally yields a self-contained electrode structure that can operate in the absence of binders or additives.[30,31] Figure 2a demonstrates the experimental configuration for the anodization process that is universally applied to both steel and brass. This setup involves low-cost processing in electrolytes using low voltages that can be achieved in a household setting (see the methods, Supporting Information). To guide efforts in processing steel and brass materials into electrodes containing redox-active materials, Raman spectroscopy (532 nm excitation, Figure 2b) and scanning electron microscopy (SEM, Figure 2c,d) were used to assess the chemical and physical characteristics of the resulting materials, respectively. Elemental analysis using energy-dispersive spectroscopy (EDS) of the processed steel and brass (Figures S1 and S2, respectively) revealed the presence of oxygen on the surface, indicating that the surfaces of both electrodes have been oxidized through the processing. Following anodization, distinct Raman signatures corresponding to T_{2g} (225 cm^{-1}, 409 cm^{-1}), E_g (290 cm^{-1}), and A_g (660 cm^{-1}) modes are observed in the case of anodized steel.[32,33] For anodized brass, one A_g

DOI: 10.1021/acsenergylett.6b00295
ACS Energy Lett. 2016, 1, 1034−1041

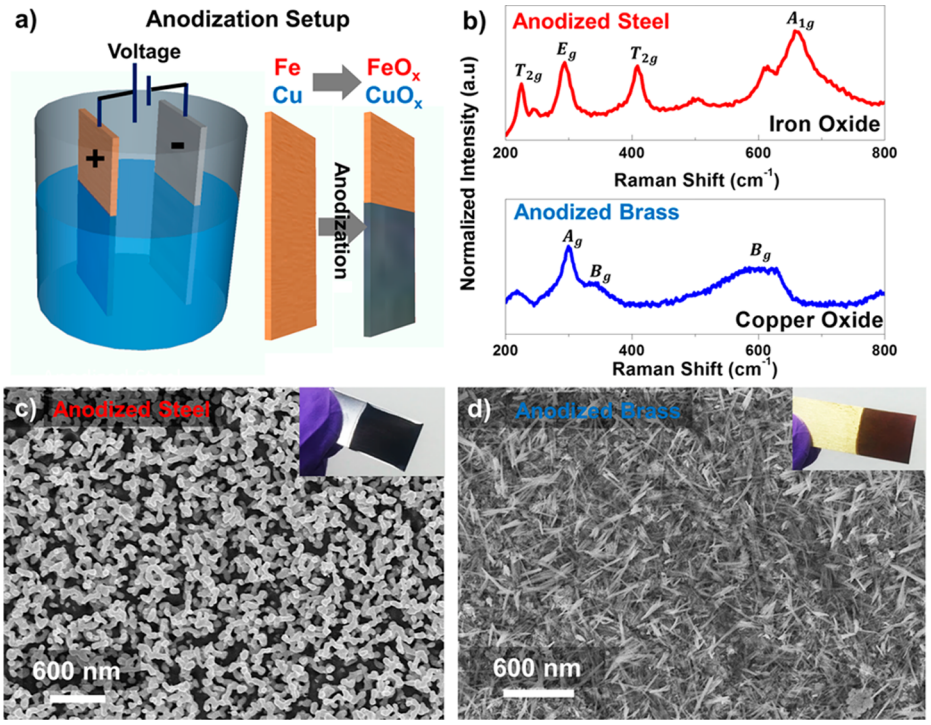

Figure 2. (a) Schematic representation of the anodization process applicable to both steel and brass electrodes. (b) Raman spectra of the treated steel and brass surfaces showing the Raman signatures of iron oxide and copper oxide. (c) SEM micrograph showing iron oxide nanorods developed on the steel surface. (Inset) Photograph of a treated steel electrode. (d) SEM micrograph showing copper oxide nanothorns developed on the steel surface. (Inset) Photograph of a treated brass electrode.

(300 cm^{-1}) mode and two B_g (337 cm^{-1}, 600 cm^{-1}) modes are observed.[34−37] This assessment confirms the capability of the anodization processes to result in the formation of iron oxide and copper oxide on the treated steel and brass, respectively. SEM micrographs shown in Figure 2c,d for the treated steel and brass surfaces indicate the presence of a nanostructured surface oxide in nanorod and nanothorn architectures, respectively. These nanostructured surface oxides are in direct contact with the metallic steel and brass surfaces, which function as effective current collectors to facilitate redox reactions of the respective oxides. As supported by recent studies,[7,24] this electrode morphology is well-suited for ultrafast cycling performance.

To individually assess the electrochemical performance of each electrode, we performed electrochemical measurements in a three-electrode configuration with the anodized scrap steel and brass as the working electrodes against a platinum or gold counter with a SCE reference (see the methods, Supporting Information). Figure 3a shows the cyclic voltammograms of the surface-activated steel electrode at scan rates of 10−500 mV/s. The voltammograms show clear anodic and cathodic peaks centered at around −0.7 and −1.1 V, respectively, which correspond to the Fe^{3+}/Fe^{2+} redox couple according to the following reaction[38]

$$Fe(OH)_2 + OH^- \leftrightarrow FeOOH + H_2O + e^-$$

This redox couple operating at negative potentials with respect to SCE is an ideal candidate for consideration as an anode for the scrap metal battery. As the voltammograms show distinct Faradaic reactions that contribute to most of the energy stored, the performance of the electrode can be assessed by determining the specific capacity (mAh/g), as shown in Figure 3b. The anodized steel electrode boasts a capacity of 270 mAh/g based on the mass of the active material. At scan rates 20 times higher, the electrode maintains a capacity of 100 mAh/g. Owing to the ultrafast nature of this redox reaction, the three-electrode performance is relevant to hybrid devices where such a device is coupled with a non-Faradaic (e.g., carbon) counterelectrode and assessed based on its specific capacitance. The specific capacitance (Figure 3b) of these electrodes ranged from 770 F/g at slow rates of 10 mV/s to 300 F/g at fast rates of 500 mV/s. In contrast to the iron oxide redox reactions of the steel electrode, the voltammograms of the brass (Figure 3c) reveal the redox electrochemistry of copper oxide at positive potentials with respect to SCE ranging from 0.2 to 0.6 V vs SCE, suggesting ideally suited pairing for the anodized steel electrodes. Due to the broad nature of the electrochemical peak(s) seen in Figure 3c, this is expected to represent an envelope of electroactive surface species comprosed of CuO, Cu_2O, CuOH, and $Cu(OH)_2$.[28] The anodized brass electrode had a specific capacity of 45 mAh/g at low scan rates of 10 mV/s and 20 mAh/g at scan rates of 500 mV/s, as represented in Figure 3d. Similar to the steel electrodes, we estimated the specific capacitance of the anodized brass electrodes to be 270 F/g (10 mV/s) to 130 F/g (500 mV/s), as shown in Figure 3d. One significant advantage of both the steel and brass electrodes is the ability to maintain >40% of the capacity at high rates even up to 500 mV/s. In both cases, this can be attributed to the nanoscale structure of the active materials that mitigates the necessity of fillers or conductive additives and enables intimate contact between the active material and the current collector. The redox peak potentials of the anodized steel and brass electrode indicate the possibility of pairing these reactions in a full cell architecture with steel anodes and brass cathodes (Figure 3e). To support the potentiodynamic cyclic voltammetry data, Figure 3f shows the galvanostatic charge−discharge

DOI: 10.1021/acsenergylett.6b00295
ACS Energy Lett. 2016, 1, 1034−1041

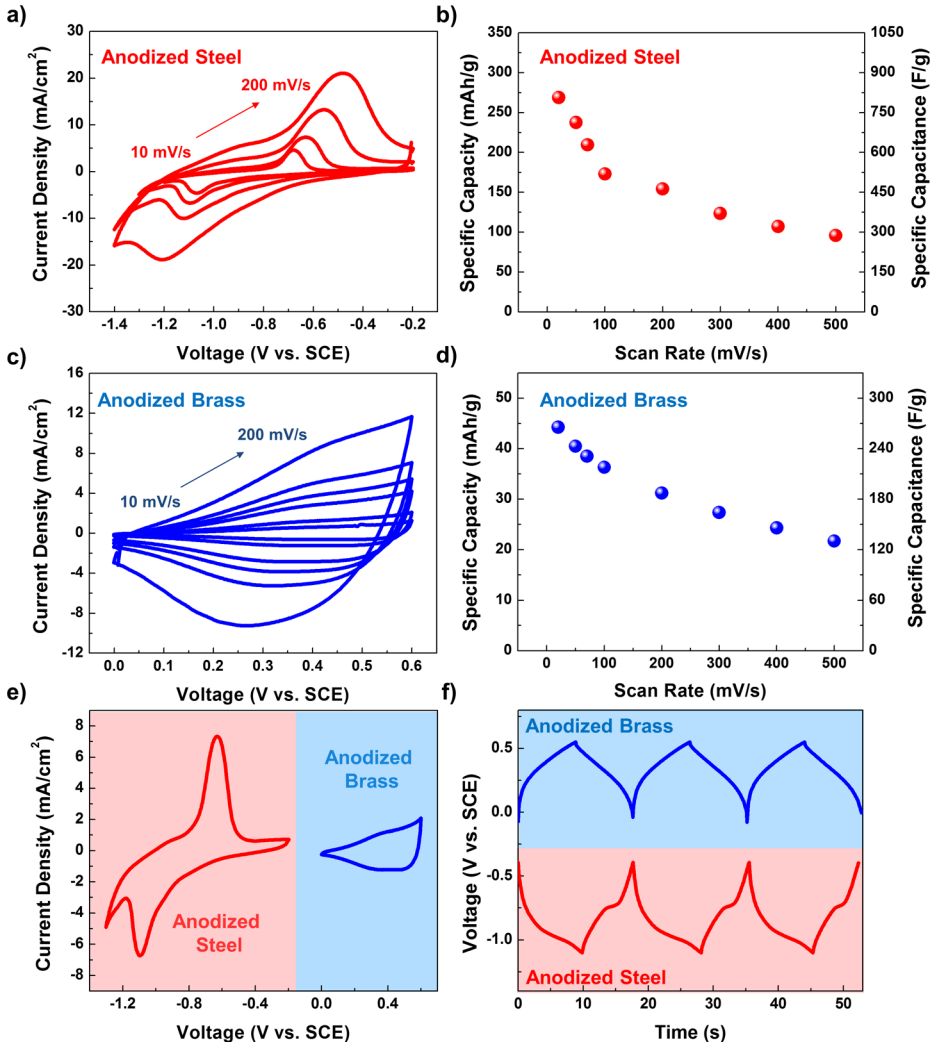

Figure 3. (a) Cyclic voltammograms of an anodized steel electrode at scan rates of 10−200 mV/s. (b) Specific capacitance and specific capacity for anodized steel calculated from cyclic voltammograms. (c) Cyclic voltammograms of an anodized brass electrode at scan rates of 10−200 mV/s. (d) Specific capacitance and specific capacity for anodized brass calculated from cyclic voltammograms. (e) Cyclic voltammograms of the anodized steel and brass electrodes showing the pairing possibility of the Fe−Cu redox couples. (f) Galvanostatic charge−discharge curves of anodized steel and anodized brass electrodes plotted vs SCE.

curves of the steel and brass electrodes where a comparison of the redox potentials indicates an overall potential window of 0.8−1.8 V when paired in a full cell architecture.

Leveraging the relative location of the redox couples in each nanostructured electrode, we used the same electrolyte system to successfully pair the iron oxide/copper oxide redox couples in a full cell battery architecture, thus producing the first ever entirely scrap-metal-derived battery as well as the first instance of pairing steel and brass materials into a battery system. Cyclic voltammetry measurements (Figure 4a) indicate reversible charge storage in the voltage window of 0.8−1.8 V in the battery. Increasing the scan rate up to 500 mV/s also demonstrates that the battery system maintains the ultrafast storage properties addressed in half-cell assessments (Figure 3). Assessing the discharge curves shown in Figure 4b, we observe a discharge capacitance of 110 F/g (discharge capacity of 16 mAh/g) at a current density of 0.5 A/g with a discharge time > 100 s.

Following the precedent set by similar paired high-rate nanomaterial batteries in recent years, especially the case of ultrafast nickel−iron batteries, for the half-cell characterizations, we provided both the specific capacity and specific capacitance values for each of our individual electrode materials. However, when these (Faradaic) electrodes are paired together with a cell potential based on the redox activity at the anode and cathode, the resulting device platform is termed a battery. However, the high rate capability of these electrodes, like many other nanostructured oxides that have been studied as pseudocapacitive materials, offers the capability to be paired with traditional electric double-layer electrodes to form hybrid capacitor devices that exhibit a capacitive response. Thus, our reporting of both specific capacity and specific capacitance allows for the broadest comparison to other relevant reports on similar materials employed in supercapacitor or battery configurations. A more in-depth discussion of where our electrodes and full cell devices fit in the broader view of energy storage is provided in the Supporting Information (Figure S3 and Table S4).[7,24,39,40]

To illustrate the stability of this paired anodized steel and brass system, we performed galvanostatic charge−discharge tests over 5000 cycles at a current density of 5 A/g (Figure 4c). After an initial electrode stabilization phase of 100 cycles, the

DOI: 10.1021/acsenergylett.6b00295
ACS Energy Lett. 2016, 1, 1034−1041

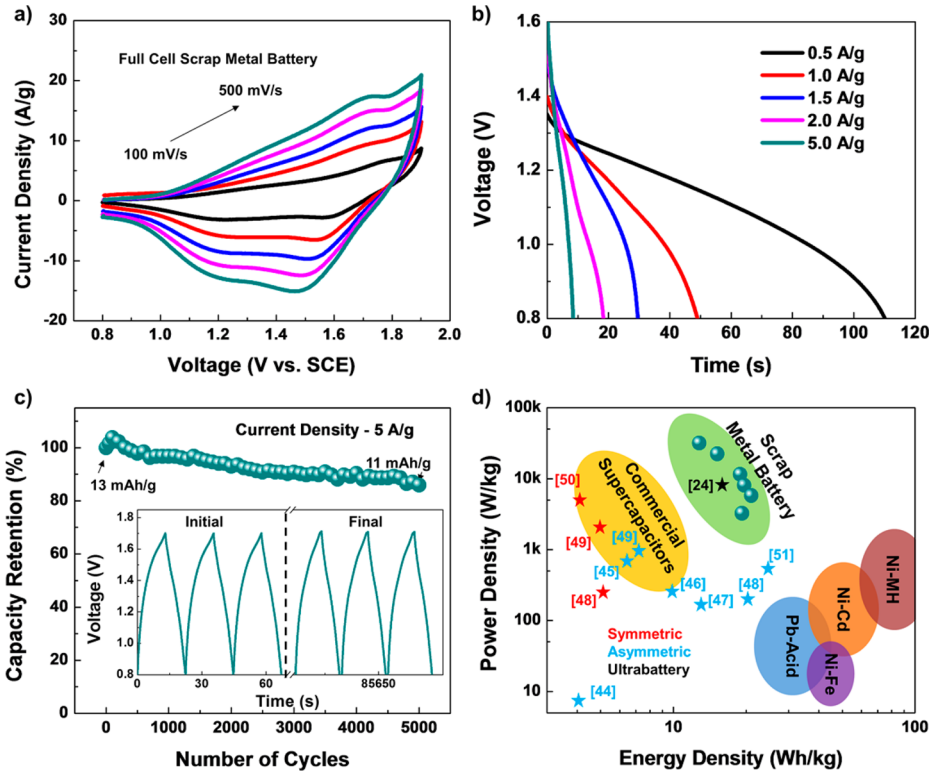

Figure 4. (a) Cyclic voltammograms of the scrap metal battery with steel anode and brass cathodes at scan rates from 100 to 500 mV/s. (b) Galvanostatic discharge curves of the a scrap metal battery at current densities from 0.5 to 5 A/g. (c) Cycling behavior of the scrap metal battery up to 5000 charge−discharge curves at a current density of 5 A/g. (Inset) Initial and near-final galvanostatic charge−discharge performance. (d) Ragone plot comparing the performance of the scrap metal battery to commercial supercapacitors and other aqueous-based battery systems along with specific references to symmetric (red stars) and asymmetric devices (blue stars) and an ultrabattery (black star) reported in the literature.

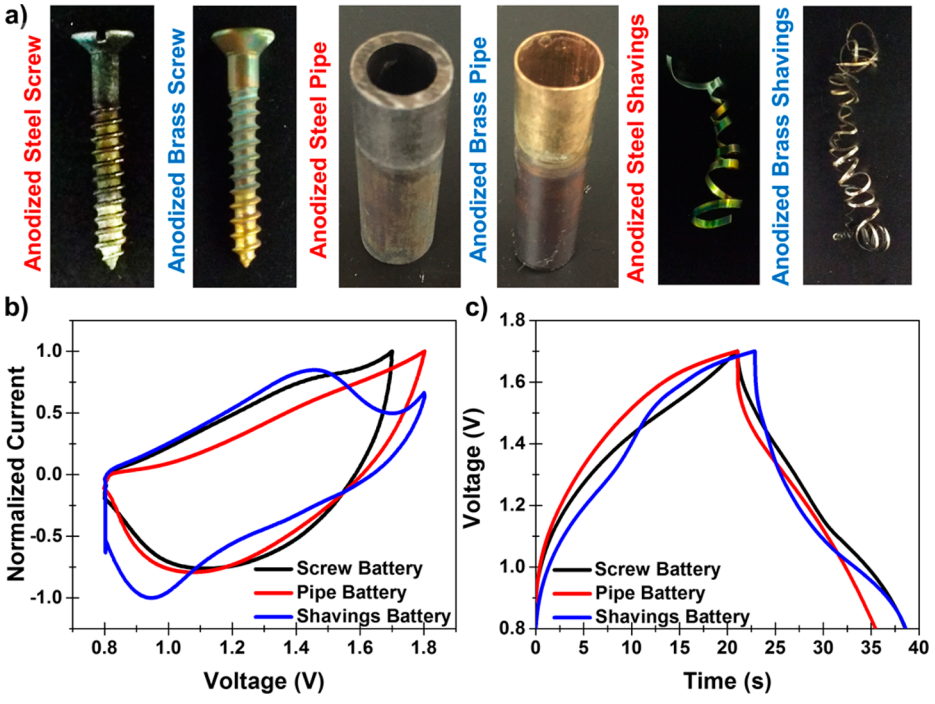

Figure 5. (a) Optical image of the anodized steel and brass screws, pipes, and shavings. (b) Cyclic voltammograms of the scrap metal batteries made from anodized steel and brass screws, pipes, and shavings. (c) Galvanostatic charge−discharge curves of the scrap metal batteries made from anodized steel and brass screws, pipes, and shavings.

DOI: 10.1021/acsenergylett.6b00295
ACS Energy Lett. 2016, 1, 1034−1041

full cell reached a stable discharge capacity. For this ultrafast scrap metal battery, the paired electrodes retained 85% of the initial capacity of 13 mAh/g even after charging and discharging the device for 5000 cycles.

EIS measurements were performed on the full cell steel−brass battery to understand the nature of the electrical connectivity of the active materials in the developed nanostructured electrodes (Figure S5). On the basis of fitting EIS data with an appropriate equivalent circuit, the scrap metal battery was determined to exhibit an equivalent series resistance of 6.23 Ω, which emphasizes a highly conductive interface between the iron oxide nanorods and copper oxide nanothorns on the steel and brass electrodes, respectively, and is important to mitigate power loss at high rate cycling conditions.

Further, to compare the performance of the ultrafast scrap metal battery to other traditional battery systems, we construct a Ragone plot from galvanostatic charge−discharge curves in Figure 4d. Our scrap metal battery has an energy density of 20 Wh/kg while functioning in the ultrafast high-power regime from 5 to 20 kW/kg. The operating voltage window of this scrap metal battery is dictated by the aqueous electrolyte used, which limits the energy density when compared to traditional Li ion batteries.[3] Whereas the energy density approaches traditional Pb acid and Ni−Fe battery systems, the ability to maintain this energy performance at high rates similar to or better than that of supercapacitors makes this an attractive energy storage system.[41−43] We note that this is compared to packaged commercial battery systems, where active mass makes up over 50% of the device mass with a specific ratio dependent upon battery size, chemistry, and so forth. However, even with such performance offsets taken into account, the broad implication of our results compared to these systems emphasizes the capability to store energy as a battery but with high power cycling capability that is important for grid coupling with renewable power sources. To further illustrate the performance of this scrap metal battery to unpackaged devices in past research reports, we compared our results to some existing literature works on hybrid devices (asymmetric and symmetric capacitors) (Figure 4d) and other paired high-rate electrode chemistries such as the Ni−Fe ultrabattery,[24,44−51] which emphasizes the high power capability and moderate energy density that is notable for the targeted grid scale integration of this steel−brass battery system.

Finally, to demonstrate the versatility of this process, we show the capability to anodize random scrap metal items such as screws, pipes, and metal shavings and then implement them as electrodes for scrap metal batteries (Figure 5). In particular Figure 5b,c shows the paired battery performance of these anodized pipes, screws, and metal shavings in true scrap metal battery architectures. In addition to demonstrating the versatility of this process, the ability to anodize screws, pipes, and other functional materials suggests the possibility of developing multifunctional batteries using this approach. Outside of simply converting scrap metals into batteries, the ability to produce energy-storing screws that could be mounted into an ion-conducting (but electrically insulating) backplane or metal pipes with integrated energy storage in the inactive materials represents systems that our work emphasizes as being feasible. As the different surface to volume ratios of these different objects will result in different amounts of surface oxide for identical anodization conditions, optimizing parameters such as time, voltage, temperature, and electrolyte concentration can account for this difference.[22,52] On this note, many types of scraps consist of large items that are not immediately useable in this type of battery architecture. However, one of the key steps in the scrap recycling process is the shredding of these larger items prior to melting, purification, and casting. For these larger items, it would be feasible to develop them into batteries after this shredding process, eliminating the energy-expensive melting and purification steps in the traditional scrap recycling process (see Table S6).

Finally, whereas we report here the specific instance of processing brass and steel into a scrap metal battery system that builds upon copper oxide and iron oxide active materials, we emphasize that this approach is not limited to this reaction pair. Chemical processes to leverage zinc[53−55] electrochemistry using brass alloys,[56,57] chromium and nickel oxide reactions in stainless steel,[7,21,22,24,58] and metal hydride and aluminum air electrochemistry using aluminum[59,60] should all be distinct possibilities. This provides a broadly generalizable platform to repurpose otherwise discarded materials into functional energy storage electrodes in a manner that can be performed in a local environment. Whereas consumer-driven development of stationary storage systems is likely to be a controversial idea based on the status quo of large-scale battery manufacturing, our work gives promise to a future vision where researchers can provide an instruction manual to a consumer, as opposed to a product, to generate local energy storage solutions. This not only bypasses the significant technological barriers to commercializing low-cost stationary storage but also gives promise to a sustainable method of repurposing abundant, low-value manufactured alloys common in a household setting into functional energy storage materials.

In summary, we demonstrate the first ever entirely scrap metal rechargeable battery as well as the first instance of pairing steel and brass materials into a battery system. Low-voltage anodization processes are developed that isolate nanostructured redox-active copper oxide and iron oxide materials from these multicomponent alloys, which we show to be well-suited for energy storage applications. The individual electrodes boast superb specific capacitance values of up to 800 and 265 F/g (270 and 45 mAh/g) for the steel and brass, respectively, and when paired into a full cell yield energy storage capability of up to 20 Wh/kg, power densities of up to 20 kW/kg, and cycling stability over 5000 cycles. As anodization is a simple process generalizable to 3-D objects, we further demonstrate the ability to use this technique to form highly accessible redox storage on the surface of commonplace steel or brass objects such as screws and shavings. This work lays the foundation to envision a sustainable route to low-cost and repurposed stationary energy storage materials. Further, inspired by the first documented reports of batteries where the materials were locally recovered, processed, and fabricated into small-scale battery systems, we present a vision that builds on the simplicity of anodization and the commonplace of brass and steels in a household setting that can enable the "scaling-down" of battery assembly in a manner that parallels the relationship of 3-D printing to large-scale centralized manufacturing processes.

■ ASSOCIATED CONTENT

Supporting Information

The Supporting Information is available free of charge on the ACS Publications website at DOI: 10.1021/acsenergylett.6b00295.

DOI: 10.1021/acsenergylett.6b00295
ACS Energy Lett. 2016, 1, 1034−1041

Experimental methods, additional compositional analysis using EDS mapping and elemental spectra of the anodized and treated steel (Figure S1) and brass (Figure S2) surfaces consisting of the developed iron oxide nanorods and copper oxide nanothorns, detailed classification of the nomenclature of the scrap metal battery (Figure S3 and Table S4), electrochemical impedance spectroscopy of the scrap metal battery (Figure S5), the steps involved in the recycling process with potential avenues for developing scrap metal batteries (Figure S6), and a list of commercially available common chemicals that can potentially be used in developing scrap metal batteries (Table S7) (PDF)

AUTHOR INFORMATION

Corresponding Author

*E-mail: cary.l.pint@vanderbilt.edu.

Author Contributions

§N.M. and A.S.W. contributed equally to this work.

Notes

The authors declare no competing financial interest.

ACKNOWLEDGMENTS

The authors would like to thank Matt McCarthy and PSC metals for useful insights into scrap metal refining procedures and on-site tours of PSC metals, a local scrap metal processing facility. We would also like to acknowledge Rizia Bardhan for use of Raman facilities. This work was supported in part by NASA EPSCoR Grant NNX13AB26A, the Vanderbilt University Discovery Grant program, and National Science Foundation graduate fellowship under grant no. 1445197.

REFERENCES

(1) Armand, M.; Tarascon, J.-M. Building Better Batteries. *Nature* **2008**, *451*, 652−657.

(2) Goodenough, J. B.; Park, K.-S. The Li-Ion Rechargeable Battery: A Perspective. *J. Am. Chem. Soc.* **2013**, *135*, 1167−1176.

(3) Tarascon, J.-M.; Armand, M. Issues and Challenges Facing Rechargeable Lithium Batteries. *Nature* **2001**, *414*, 359−367.

(4) Scrosati, B. History of Lithium Batteries. *J. Solid State Electrochem.* **2011**, *15*, 1623−1630.

(5) Pancaldi, G. Electricity and Life. Volta's Path to the Battery. *Hist. Stud. Phys. Biol. Sci.* **1990**, *21*, 123−160.

(6) Chakkaravarthy, C.; Periasamy, P.; Jegannathan, S.; Vasu, K. The Nickel/Iron Battery. *J. Power Sources* **1991**, *35*, 21−35.

(7) Wang, H.; Liang, Y.; Gong, M.; Li, Y.; Chang, W.; Mefford, T.; Zhou, J.; Wang, J.; Regier, T.; Wei, F.; Dai, H. An Ultrafast Nickel−Iron Battery from Strongly Coupled Inorganic Nanoparticle/Nanocarbon Hybrid Materials. *Nat. Commun.* **2012**, *3*, 917.

(8) Shukla, A.; Ravikumar, M.; Balasubramanian, T. Nickel/Iron Batteries. *J. Power Sources* **1994**, *51*, 29−36.

(9) Dunn, B.; Kamath, H.; Tarascon, J.-M. Electrical Energy Storage for the Grid: A Battery of Choices. *Science* **2011**, *334*, 928−935.

(10) Chen, H.; Cong, T. N.; Yang, W.; Tan, C.; Li, Y.; Ding, Y. Progress in Electrical Energy Storage System: A Critical Review. *Prog. Nat. Sci.* **2009**, *19*, 291−312.

(11) Leung, P.; Li, X.; Ponce de León, C.; Berlouis, L.; Low, C. J.; Walsh, F. C. Progress in Redox Flow Batteries, Remaining Challenges and their Applications in Energy Storage. *RSC Adv.* **2012**, *2*, 10125−10156.

(12) Kim, H.; Boysen, D. A.; Newhouse, J. M.; Spatocco, B. L.; Chung, B.; Burke, P. J.; Bradwell, D. J.; Jiang, K.; Tomaszowska, A. A.; Wang, K.; et al. Liquid Metal Batteries: Past, Present, and Future. *Chem. Rev.* **2013**, *113*, 2075−2099.

(13) Campbell, T.; Williams, C.; Ivanova, O.; Garrett, B. Could 3D Printing Change the World. *Technologies, Potential, and Implications of Additive Manufacturing*; Atlantic Council: Washington, DC, 2011.

(14) Ambrosi, A.; Pumera, M. 3D-Printing Technologies for Electrochemical Applications. *Chem. Soc. Rev.* **2016**, *45*, 2740−2755.

(15) Petrick, I. J.; Simpson, T. W. 3D Printing Disrupts Manufacturing: How Economies of One Create New Rules of Competition. *Res. Technol. Manage.* **2013**, *56*, 12−16.

(16) *Mineral Commodities Summary 2015*; US Department of the Interior, US Geological Survey: Reston, VA, 2015.

(17) Goonan, T. G. *Copper Recycling in the United States in 2004*; US Department of the Interior, US Geological Survey: Reston, VA, 2010.

(18) Ayres, R. U. Metals Recycling: Economic and Environmental Implications. *Resour. Conserv. Recycl.* **1997**, *21*, 145−173.

(19) Damuth, R. J. *Iron and Steel Scrap: Accumulation and Availability as of December 31, 2009* US Institute of Scrap Recycling Industries, 2010.

(20) Wu, X.; Bai, H.; Zhang, J.; Chen, F. e.; Shi, G. Copper Hydroxide Nanoneedle and Nanotube Arrays Fabricated by Anodization of Copper. *J. Phys. Chem. B* **2005**, *109*, 22836−22842.

(21) Macak, J. M.; Tsuchiya, H.; Schmuki, P. High-Aspect-Ratio TiO_2 Nanotubes by Anodization of Titanium. *Angew. Chem., Int. Ed.* **2005**, *44*, 2100−2102.

(22) Hang, R.; Liu, Y.; Zhao, L.; Gao, A.; Bai, L.; Huang, X.; Zhang, X.; Tang, B.; Chu, P. K. Fabrication of Ni-Ti-O Nanotube Arrays by Anodization of NiTi Alloy and Their Potential Applications. *Sci. Rep.* **2014**, *4*, 7547.

(23) Kim, J.-H.; Zhu, K.; Yan, Y.; Perkins, C. L.; Frank, A. J. Microstructure and Pseudocapacitive Properties of Electrodes Constructed of Oriented NiO-TiO_2 Nanotube Arrays. *Nano Lett.* **2010**, *10*, 4099−4104.

(24) Sarkar, D.; Shukla, A. K.; Sarma, D. D. Substrate Integrated Nickel-Iron Ultra-Battery with Extraordinarily Enhanced Performances. *ACS Energy Lett.* **2016**, *1*, 82−88.

(25) Jiang, W.; Liang, F.; Wang, J.; Su, L.; Wu, Y.; Wang, L. Enhanced Electrochemical Performances of FeO_x−Graphene Nanocomposites as Anode Materials for Alkaline Nickel−Iron Batteries. *RSC Adv.* **2014**, *4*, 15394−15399.

(26) Lei, D.; Lee, D.-C.; Magasinski, A.; Zhao, E.; Steingart, D.; Yushin, G. Performance Enhancement and Side Reactions in Rechargeable Nickel−Iron Batteries with Nanostructured Electrodes. *ACS Appl. Mater. Interfaces* **2016**, *8*, 2088−2096.

(27) Lu, W.; Sun, Y.; Dai, H.; Ni, P.; Jiang, S.; Wang, Y.; Li, Z.; Li, Z. CuO Nanothorn Arrays on Three-Dimensional Copper Foam as an Ultra-Highly Sensitive and Efficient Nonenzymatic Glucose Sensor. *RSC Adv.* **2016**, *6*, 16474−16480.

(28) Shinde, S.; Dubal, D.; Ghodake, G.; Kim, D.; Fulari, V. Nanoflower-Like CuO/$Cu(OH)_2$ Hybrid Thin Films: Synthesis and Electrochemical Supercapacitive Properties. *J. Electroanal. Chem.* **2014**, *732*, 80−85.

(29) Golev, A.; Corder, G. Modelling Metal Flows in the Australian Economy. *J. Cleaner Prod.* **2016**, *112*, 4296−4303.

(30) Sagu, J. S.; Wijayantha, K. U.; Bohm, M.; Bohm, S.; Kumar Rout, T. Anodized Steel Electrodes for Supercapacitors. *ACS Appl. Mater. Interfaces* **2016**, *8*, 6277−6285.

(31) Qin, C.; Zhang, Y.; Wang, Z.; Xiong, H.; Yu, H.; Zhao, W. One-Step Synthesis of CuO@ Brass Foil by Dealloying Method For Low-Cost Flexible Supercapacitor Electrodes. *J. Mater. Sci.: Mater. Electron.* **2016**, *27*, 9206−9215.

(32) Song, K.; Lee, Y.; Jo, M. R.; Nam, K. M.; Kang, Y.-M. Comprehensive Design of Carbon-Encapsulated Fe_3O_4 Nanocrystals and Their Lithium Storage Properties. *Nanotechnology* **2012**, *23*, 505401.

(33) Sirivisoot, S.; Harrison, B. S. Magnetically Stimulated Ciprofloxacin Release From Polymeric Microspheres Entrapping Iron Oxide Nanoparticles. *Int. J. Nanomed.* **2015**, *10*, 4447.

(34) Akgul, F. A.; Akgul, G.; Yildirim, N.; Unalan, H. E.; Turan, R. Influence of Thermal Annealing on Microstructural, Morphological,

DOI: 10.1021/acsenergylett.6b00295
ACS Energy Lett. 2016, 1, 1034−1041

Optical Properties and Surface Electronic Structure of Copper Oxide Thin Films. *Mater. Chem. Phys.* **2014**, *147*, 987−995.
(35) Wang, S.; Huang, Q.; Wen, X.; Li, X.-y.; Yang, S. Thermal Oxidation of Cu_2S Nanowires: A Template Method for the Fabrication of Mesoscopic Cu_xO (x= 1, 2) Wires. *Phys. Chem. Chem. Phys.* **2002**, *4*, 3425−3429.
(36) Fuentes, S.; Zárate, R.; Munoz, P.; DÍaz-Droguett, D. E. Formation of Hierarchical CuO Nanowires on a Copper Surface via a Room-Temperature Solution-Immersion Process. *J. Chil. Chem. Soc.* **2010**, *55*, 147−149.
(37) Lin, Y.-G.; Hsu, Y.-K.; Chen, S.-Y.; Chen, L.-C.; Chen, K.-H. Microwave-Activated CuO Nanotip/ZnO Nanorod Nanoarchitectures for Efficient Hydrogen Production. *J. Mater. Chem.* **2011**, *21*, 324−326.
(38) Doyle, R. L.; Godwin, I. J.; Brandon, M. P.; Lyons, M. E. Redox and Electrochemical Water Splitting Catalytic Properties of Hydrated Metal Oxide Modified Electrodes. *Phys. Chem. Chem. Phys.* **2013**, *15*, 13737−13783.
(39) Simon, P.; Gogotsi, Y.; Dunn, B. Where do batteries end and supercapacitors begin? *Science* **2014**, *343*, 1210−1211.
(40) Brousse, T.; Bélanger, D.; Long, J. W. To be or not to be pseudocapacitive? *J. Electrochem. Soc.* **2015**, *162*, A5185−A5189.
(41) Nyström, G.; Marais, A.; Karabulut, E.; Wågberg, L.; Cui, Y.; Hamedi, M. M. Self-assembled three-dimensional and compressible interdigitated thin-film supercapacitors and batteries. *Nat. Commun.* **2015**, *6*, 7259.
(42) Halpert, G. Past developments and the future of nickel electrode cell technology. *J. Power Sources* **1984**, *12*, 177−192.
(43) Padbury, R.; Zhang, X. Lithium−oxygen batteries—limiting factors that affect performance. *J. Power Sources* **2011**, *196*, 4436−4444.
(44) Lu, X.; Yu, M.; Zhai, T.; Wang, G.; Xie, S.; Liu, T.; Liang, C.; Tong, Y.; Li, Y. High energy density asymmetric quasi-solid-state supercapacitor based on porous vanadium nitride nanowire anode. *Nano Lett.* **2013**, *13*, 2628−2633.
(45) Brousse, T.; Bélanger, D. A Hybrid Fe_3O_4 MnO_2 Capacitor in Mild Aqueous Electrolyte. *Electrochem. Solid-State Lett.* **2003**, *6*, A244−A248.
(46) Lin, Y.-P.; Wu, N.-L. Characterization of $MnFe_2O_4/LiMn_2O_4$ aqueous asymmetric supercapacitor. *J. Power Sources* **2011**, *196*, 851−854.
(47) Shanmugavani, A.; Selvan, R. K. Synthesis of $ZnFe_2O_4$ nanoparticles and their asymmetric configuration with $Ni(OH)_2$ for a pseudocapacitor. *RSC Adv.* **2014**, *4*, 27022−27029.
(48) Wang, R.; Yan, X.; Lang, J.; Zheng, Z.; Zhang, P. A hybrid supercapacitor based on flower-like $Co(OH)_2$ and urchin-like VN electrode materials. *J. Mater. Chem. A* **2014**, *2*, 12724−12732.
(49) Cottineau, T.; Toupin, M.; Delahaye, T.; Brousse, T.; Belanger, D. Nanostructured transition metal oxides for aqueous hybrid electrochemical supercapacitors. *Appl. Phys. A: Mater. Sci. Process.* **2006**, *82*, 599−606.
(50) Lu, X.; Wang, G.; Zhai, T.; Yu, M.; Xie, S.; Ling, Y.; Liang, C.; Tong, Y.; Li, Y. Stabilized TiN nanowire arrays for high-performance and flexible supercapacitors. *Nano Lett.* **2012**, *12*, 5376−5381.
(51) Jin, W.-H.; Cao, G.-T.; Sun, J.-Y. Hybrid supercapacitor based on MnO_2 and columned FeOOH using Li_2SO_4 electrolyte solution. *J. Power Sources* **2008**, *175*, 686−691.
(52) Gao, Z.-D.; Han, Y.; Wang, Y.; Xu, J.; Song, Y.-Y. One-Step to Prepare Self-Organized Nanoporous NiO/TiO_2 Layers and its Use in Non-Enzymatic Glucose Sensing. *Sci. Rep.* **2013**, *3*, 3323.
(53) Gupta, T.; Kim, A.; Phadke, S.; Biswas, S.; Luong, T.; Hertzberg, B. J.; Chamoun, M.; Evans-Lutterodt, K.; Steingart, D. A. Improving the Cycle Life of a High-Rate, High-Potential Aqueous Dual-Ion Battery Using Hyper-Dendritic Zinc and Copper Hexacyanoferrate. *J. Power Sources* **2016**, *305*, 22−29.
(54) Chamoun, M.; Hertzberg, B. J.; Gupta, T.; Davies, D.; Bhadra, S.; Van Tassell, B.; Erdonmez, C.; Steingart, D. A. Hyper-Dendritic Nanoporous Zinc Foam Anodes. *NPG Asia Mater.* **2015**, *7*, e178.
(55) Zamarayeva, A. M.; Gaikwad, A. M.; Deckman, I.; Wang, M.; Khau, B.; Steingart, D. A.; Arias, A. C. Fabrication of a High-Performance Flexible Silver−Zinc Wire Battery. *Adv. Electron. Mater.* **2016**, *2*, 1500296.
(56) Mainar, A. R.; Leonet, O.; Bengoechea, M.; Boyano, I.; de Meatza, I.; Kvasha, A.; Guerfi, A.; Alberto Blázquez, J. Alkaline Aqueous Electrolytes for Secondary Zinc−Air Batteries: An Overview. *Int. J. Energy Res.* **2016**, *40*, 1032−1049.
(57) Park, J.; Park, M.; Nam, G.; Lee, J. s.; Cho, J. All-Solid-State Cable-Type Flexible Zinc−Air Battery. *Adv. Mater.* **2015**, *27*, 1396−1401.
(58) Zeng, Y.; Zhou, X.; An, L.; Wei, L.; Zhao, T. A High-Performance Flow-Field Structured Iron-Chromium Redox Flow Battery. *J. Power Sources* **2016**, *324*, 738−744.
(59) Zidan, R. A.; Takara, S.; Hee, A. G.; Jensen, C. M. Hydrogen Cycling Behavior of Zirconium and Titanium−Zirconium-Doped Sodium Aluminum Hydride. *J. Alloys Compd.* **1999**, *285*, 119−122.
(60) Li, Q.; Bjerrum, N. J. Aluminum as Anode for Energy Storage and Conversion: A Review. *J. Power Sources* **2002**, *110*, 1−10.

DOI: 10.1021/acsenergylett.6b00295
ACS Energy Lett. 2016, 1, 1034−1041